Rare Metal Materials and Engineering
Volume 53, Issue 10, October 2024
Available online at www.rmme.ac.cn

Science Press

Cite this article as: Ma Kai, Feng Li, Zhao Yanchun, et al. Microstructure and Wear Resistance Properties of FeCrAlCu(Ni, Co) HEA Coatings Synthesized by Laser Remelting[J]. Rare Metal Materials and Engineering, 2024, 53(10): 2747-2754. DOI: 10.12442/j.issn.1002-185X.20240095.

ARTICLE

Microstructure and Wear Resistance Properties of FeCrAlCu(Ni, Co) HEA Coatings Synthesized by Laser Remelting

Ma Kai[1,2], Feng Li[1,2], Zhao Yanchun[1,2], Liu Jianjun[1,2]

[1] School of Materials Science and Technology, Lanzhou University of Technology, Lanzhou 730050, China; [2] State Key Laboratory of Advanced Processing and Recycling of Nonferrous Metals, Lanzhou University of Technology, Lanzhou 730050, China

Abstract: FeCrAlCu, FeCrAlCuNi, FeCrAlCuCo, and FeCrAlCuNiCo high-entropy alloy (HEA) coatings were synthesized on the surface of 45# steel through cold spraying-assisted laser remelting. Results reveal that all four HEA coatings are composed of face-centered cubic+body-centered cubic phases. Additionally, the microstructure of the coatings consists of columnar dendrites. With the simultaneous addition of both Ni and Co elements, the columnar dendritic grains are gradually refined in the coating. Moreover, the FeCrAlCuNiCo HEA coating exhibits excellent friction performance with the coating hardness of 5847.7 MPa, friction factor of 0.45, and wear rate of 3.72×10^{-5} $mm^3\cdot N^{-1}\cdot m^{-1}$. The predominant wear mechanism is the adhesive wear and abrasive wear.

Key words: laser remelting; high-entropy alloy coating; wear mechanism; abrasion resistance

High-entropy alloys (HEAs) are unique metallic materials with five or more elements in specific proportions[1–2]. Moreover, HEAs exhibit high chemical inhomogeneity and thermodynamic stability. Compared with conventional metal alloys, HEAs exhibit excellent performance in numerous aspects, including hardness, wear resistance, and corrosion resistance[3–8]. These unique performance characteristics of HEAs broaden their applications in surface engineering[9–11].

Laser remelting is a commonly used surface treatment technique owing to its regionally controllable modification, minimal thermal deformation, and limited impact on the internal toughness. Additionally, laser remelting can eliminate defects, such as pores and cracks, within the cold-sprayed coatings, increase grain boundary density, refine grain structure, and enhance the bonding strength of coatings[12–13]. Cao et al[14] used laser cladding technique to prepare FeCrNiCoMoCuBSi HEA coatings on the surface of 316L stainless steel. The results revealed that the cladding layer mainly consisted of face-centered cubic (fcc) solid solution phases and $(Fe, Cr)_2B$ phases. The microstructure of the layer was characterized by reed-like dendrites, whereas the planar crystals in the bonding zone exhibited excellent metallurgical bonding with the substrate. Moreover, the cladding layer has average $HV_{0.2}$ hardness of 6860 MPa, which is 3.5 times higher than that of the substrate. Additionally, the cladding layer has lower friction coefficient and less wear volume than the substrate under different loads. These results all indicate that the cladding layer has better wear resistance, compared with the substrate. Furthermore, Zhang et al[15] used laser cladding technique to prepare $FeCrNiCoMnB_x$ HEA coatings. The results indicated that the coatings consisted of fcc phases and borides. When $x\leqslant0.75$, the predominant borides were the $(Cr, Fe)_2B$ phase; however, when $x=1$, a significant amount of $(Fe, Cr)_2B$ phase was generated. With the increase in boron content, the quantity of borides in the coating is increased, leading to higher hardness and enhanced wear resistance performance. Additionally, Liu et al[16] used laser cladding technique to synthesize $AlCoCrFeNiSi_x$ HEA coatings on the surface of AISI 304 stainless steel. The results revealed that the coatings consisted of body-centered cubic (bcc) solid solution grains. With the increase in Si content, the substitutional solid solution of Si atoms induces lattice contraction, leading to gradual grain refinement. Nano-sized spherical AlNi phases dissolve within the grains, whereas a small number of $Cr_{23}C_6$ carbides are precipitated along the grain boundaries. These changes in microstructure jointly increase the microhardness of the coating and the maximum microhardness $HV_{0.3}$ reaches 8311.4 MPa. Moreover, Shi et

Received date: February 27, 2024
Foundation item: Supported by China National Nuclear Power Plant Operation (QS4FY-22003224)
Corresponding author: Feng Li, Ph. D., Professor, School of Materials Science and Engineering, Lanzhou University of Technology, Lanzhou 730050, P. R. China, E-mail: fenglills@lut.edu

al[17] used the laser cladding method to synthesize in-situ NiCoCrMnFe HEA coatings on H13 tool steel. The results indicated that HEA coatings with thickness of 0.6 mm were formed, comprising a single-phase fcc solid solution. The microhardness of the cladding layer exceeded 4900 MPa, which is more than 2.5 times higher than that of the untreated substrate. No microcracks could be observed around the indentation. Furthermore, under similar friction conditions, the average wear track width of the cladding layer decreased from 0.71 mm (substrate) to 0.48 mm (HEA coating). Consequently, the wear rate of the cladding layer decreased by 63.2%, compared with that of the substrate.

In this research, Ni and Co, as transition metal elements, were introduced into the FeCrAlCu HEA to manufacture a cost-effective HEA coating with excellent properties. The addition of these elements significantly enhanced the strength and hardness of FeCrAlCu(Ni, Co) HEA coatings through crystal structure modification. Additionally, the modified FeCrAlCu(Ni, Co) HEA coatings were prepared on the surface of 45# steel using the cold spray-assisted laser remelting technique[18–20]. The effects of Ni and Co contents on the microstructure and properties of FeCrAlCu(Ni, Co) HEAs were also investigated.

1 Experiment

A pre-fabricated metal hybrid coating was initially prepared on the surface of 45# steel through the cold spraying method. Subsequently, dense HEA coatings were fabricated via laser remelting. High-purity (>99.5%) raw materials were used in the experiment, and they were proportionally mixed according to specified ratios followed by mechanical blending for 4 h using the powder mixer to serve as the cold-sprayed feedstock. Before spraying, the substrate surface was cleaned in anhydrous ethanol through ultrasonic cleaning for the removal of oil and other impurities. Then, sandblasting was conducted to roughen the substrate surface. Cold-sprayed coatings were prepared using the low-pressure cold spraying system (GDU-3-15, Belarusian State University). The cold spraying process parameters are shown in Table 1. FeCrAlCu(Ni, Co) HEA coatings were prepared using the fiber laser device (YLS-4000) for laser remelting. The laser remelting process parameters are listed in Table 2.

The phase structures of the cold-sprayed mixed powder coating and laser-remelted HEA coating were analyzed via X-ray diffractometer (XRD, D/MAX2500PC) under the conditions of scanning speed of 4°/min, step size of 0.02°, accelerating voltage of 40 kV, current of 40 mA, and diffraction angle of 20° – 90°. The microstructure of HEA coating surface was examined via field emission scanning electron microscope (SEM, TESCAN MIRA3) and field emission transmission electron microscopy (TEM, Talos F200S 200Kev) with scanning step size of 9 μm. Additionally, the microstructure of the coatings was characterized via electron backscattered diffractometer (EBSD, ZEISS EVO MA10) with scanning step size of 9 μm. EBSD images were analyzed and processed using the Channel 5 software. Selected area electron diffraction (SAED) analysis was also conducted. The Vickers hardness of the samples was measured using the microhardness tester (HV-1000) with the load of 0.5 N. To assess the microstructure of HEA coating surface, 15 points were selected for data acquirement, and their average value was calculated to determine the surface hardness. The friction performance of HEA coatings under dry friction conditions was evaluated by CSM friction and wear machine. The friction coating dimension was 20 mm×20 mm×5 mm. Alumina balls (*Φ*6 mm) served as the counter specimen. The wear volume of sample wear marks after friction experiments was measured by the laser confocal (OLS5000). The friction test parameters were set as follows: test load of 7.5 N, friction stroke of 3 mm, sliding frequency *f* of 3 Hz, and test duration of 20 min. The wear rate of HEA coating can be calculated by Eq.(1)[21], as follows:

$$\sigma = \frac{V}{\Sigma W} = \frac{AL}{2FTfL} \quad (1)$$

where σ is the wear rate ($mm^3 \cdot N^{-1} \cdot m^{-1}$), V represents the volume of friction skid mark, W is the accumulated frictional work (N·m), A is the cross-sectional area of wear, L is the abrasion mark length (mm), F is the applied load force (N), T is the friction duration, and f is the sliding frequency (Hz).

Table 1 Process parameters of cold spraying

Parameter	Value
Working gas	Compressed air
Temperature/°C	500
Shielding gas/L·min^{-1}	0.7–0.8
Spraying distance/mm	10–20
Spraying speed/m·s^{-1}	0.4–0.6

Table 2 Process parameters of laser remelting

Parameter	Value
Power/W	2400
Scanning speed/mm·s^{-1}	400
Shielding gas/L·min^{-1}	0.7–0.8
Light spot diameter/mm	15–20
Overlapping ratio/%	40–60

2 Results and Discussion

2.1 Microstructure and phase structure of FeCrAlCu(Ni, Co) HEA coatings

XRD patterns of FeCrAlCu(Ni, Co) HEA coatings are shown in Fig. 1, revealing that the FeCrAlCu(Ni, Co) HEA coatings consist of fcc and bcc phases. With the separate addition of Ni and Co, the intensity of diffraction peaks of fcc phase is almost unchanged, whereas that of bcc phase is increased. With the simultaneous addition of Ni and Co, the intensity of diffraction peak of fcc phase is decreased, whereas that of bcc phase reaches the maximum value. Consequently, the peak intensities of the bcc and fcc phases in FeCrAlCu(Ni, Co) HEA coatings are varied with Ni and Co con-

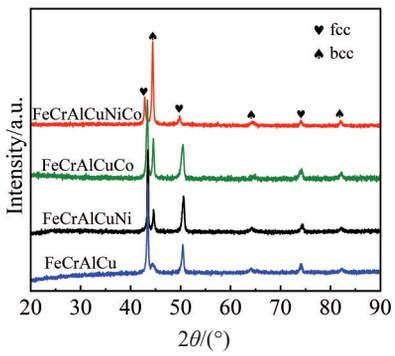

Fig.1 XRD patterns of FeCrAlCu(Ni, Co) HEA coatings

tents[22–23]. According to the correlation between diffraction peak intensity and mass, it can be concluded that the bcc phase content of FeCrAlCuNiCo HEA coating is the highest.

Fig. 2 shows SEM images of FeCrAlCu(Ni, Co) HEA coating surfaces. The FeCrAlCu HEA coating mainly consists of columnar dendrites (Fig. 2a). The FeCrAlCuNi and FeCrAlCuCo HEA coatings exhibit numerous dendrites and well-defined grain boundaries (Fig. 2b – 2c). The FeCrAlCuNiCo HEA coating exhibits columnar dendritic structures (Fig. 2d). Additionally, the dendritic structure has a larger spacing of the secondary dendritic arms. During laser remelting, the upper part of the melt pool rapidly transfers to the surrounding area, the growth direction of the nucleus in the upper part of the melt pool is unlimited, and the lower part of the melt pool forms a temperature gradient. Thus, heat transfers to the substrate, which causes the formation of columnar dendritic crystals after the crystals receive the transferred heat.

Fig.3 and Fig.4 show EBSD images and average grain sizes of FeCrAlCu(Ni, Co) HEA coating surfaces, respectively. According to Fig. 4, the average grain sizes of FeCrAlCu, FeCrAlCuNi, FeCrAlCuCo, and FeCrAlCuNiCo HEA coatings are 148.5, 134.5, 110.4, and 85.8 μm, respectively. The grain sizes in the coatings are gradually decreased with the increase in Ni and Co contents. The grain refinement effect in the coating may be attributed to the solute atoms which are solidly dissolved at the grain boundaries during the laser remelting process, thereby hindering the grain growth. It is possible that when the content of solute atoms exceeds a certain threshold, the grain refinement is promoted.

Fig. 5 shows the bright-field TEM image and SAED patterns of FeCrAlCuNiCo HEA coating prepared by laser remelting. Fig. 5a reveals the dendritic bcc phase and interdendritic fcc phase structures. Black stripes of nanoscale precipitates can be observed within the dendrites. Fig.6 shows EDS element mappings of FeCrAlCuNiCo HEA coating, which confirms that these precipitates are mainly composed of AlNi and AlCo phases, and their mixing enthalpies are −22 and − 19 kJ/mol, respectively. During the solidification process, the Cr-, Fe-, Ni-, and Co-enriched dendritic zones with bcc structure are firstly nucleated from the liquid. With the further growth of dendrites, the Al and Cu atoms deviate from the dendritic zone, the fcc AlCu phase-enriched dendrites are formed, and the bcc dendritic region consisting of AlNi and AlCo is also generated.

2.2 Mechanical properties of FeCrAlCu(Ni, Co) HEA coatings

The excellent properties of FeCrAlCu(Ni, Co) HEA coatings prepared by cold spraying-assisted laser remelting mainly originate from the HEA lattice distortion effect, and the distortion degree of the crystal lattice can be expressed through the lattice strain ε[24], as follows:

$$\varepsilon=\Delta a/a_0 \quad (2)$$

$$\Delta a=|a-a_0| \quad (3)$$

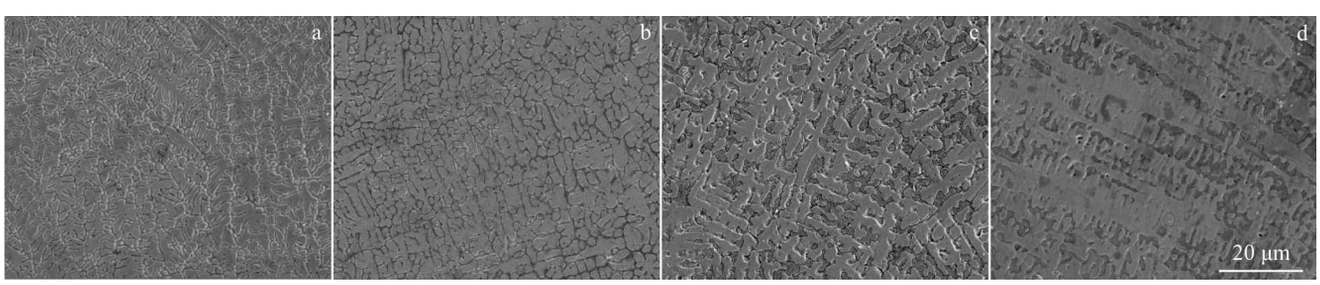

Fig.2 SEM images of FeCrAlCu(Ni, Co) HEA coating surfaces: (a) FeCrAlCu; (b) FeCrAlCuNi; (c) FeCrAlCuCo; (d) FeCrAlCuNiCo

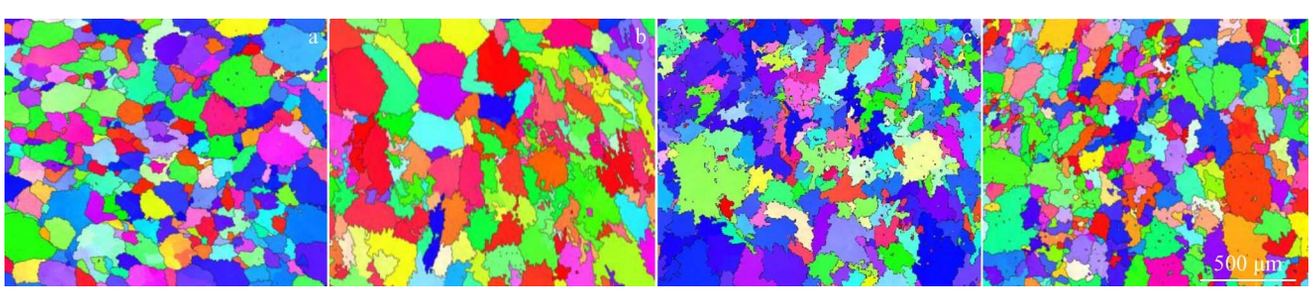

Fig.3 EBSD images of FeCrAlCu(Ni, Co) HEA coating surfaces: (a) FeCrAlCu; (b) FeCrAlCuNi; (c) FeCrAlCuCo; (d) FeCrAlCuNiCo

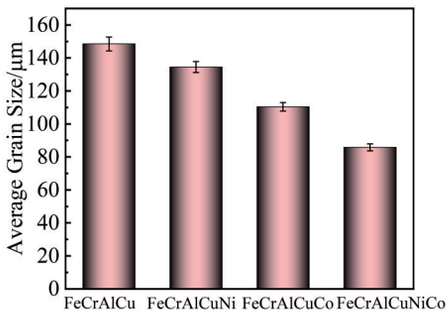

Fig.4 Average grain sizes of FeCrAlCu(Ni, Co) HEA coatings

where a and a_0 are the lattice constants of the actual and ideal lattice point formations, respectively. When the Ni and Co contents increases, the lattice strain ε of the fcc and bcc phases is increased with the increase in atomic size difference δ. According to calculation results, the lattice strain ε of bcc and fcc phases of FeCrAlCuNiCo HEA coating is 0.84% and 3.87%, respectively. After Ni and Co are simultaneously added into the HEA coating, the atomic size difference δ of FeCrAlCuNiCo HEA coating is the largest. The greater the lattice distortion degree, the more obvious the solid-solution strengthening of bcc phase.

Fig. 7a shows the hardness of FeCrAlCu(Ni, Co) HEA coatings. It can be seen that the hardness HV of FeCrAlCuNiCo HEA coatings is 5847.7 MPa. This great increment is attributed to various factors, such as the crystal structure of the coatings, fine-grain reinforcement, and solid-solution reinforcement. With the increase in Ni and Co content, lattice strain is generated in the FeCrAlCuNiCo HEA coating synthesized by laser remelting. Additionally, the solid solution strengthening is sufficient, the coating hardness becomes large, the density of fcc phase (111) is larger than that of bcc phase (110), and the value of Berth vector of fcc phase is smaller than that of bcc phase. The resistance against dislocation initiation is smaller on (111) surface, and therefore the plastic deformation easily occurs. The addition of Ni and Co atoms can increase the atomic size difference of the coating, cause the lattice distortion, and enhance the solid solution strengthening effect of the coating.

Fig. 7b shows the friction coefficients of FeCrAlCu(Ni, Co) HEA coatings. It can be seen that the friction coefficient of

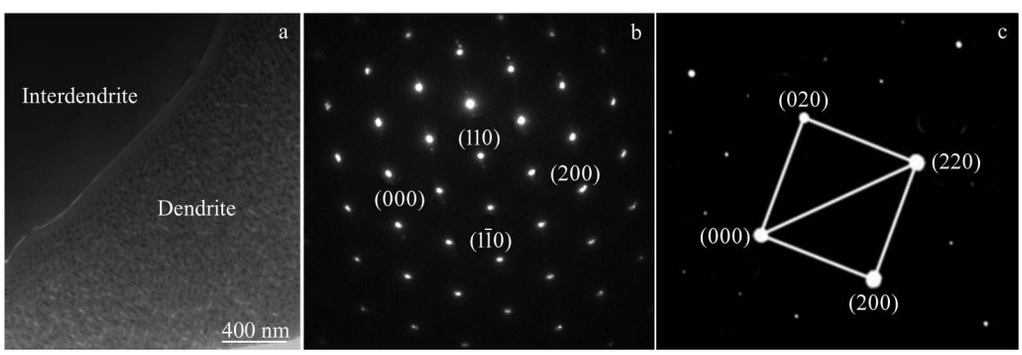

Fig.5 Bright-field TEM image of FeCrAlCuNiCo HEA coating (a); SAED patterns of interdendrite (b) and dendrite (c) in Fig.5a

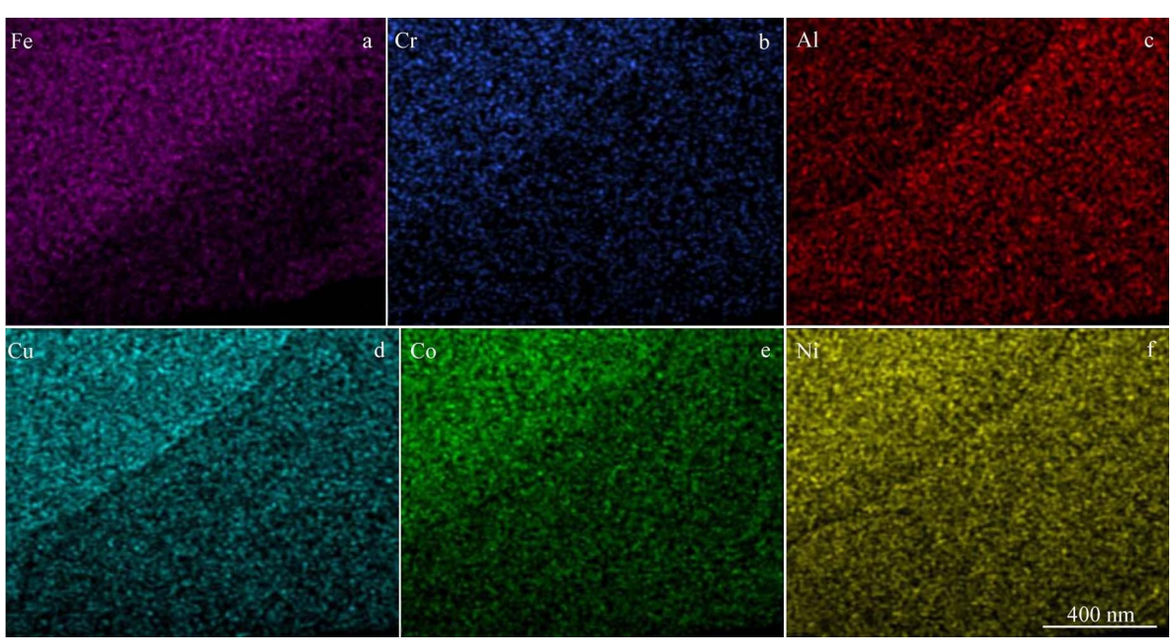

Fig.6 EDS element mappings of FeCrAlCuNiCo HEA coating: (a) Fe, (b) Cr, (c) Al, (d) Cu, (e) Co, and (f) Ni

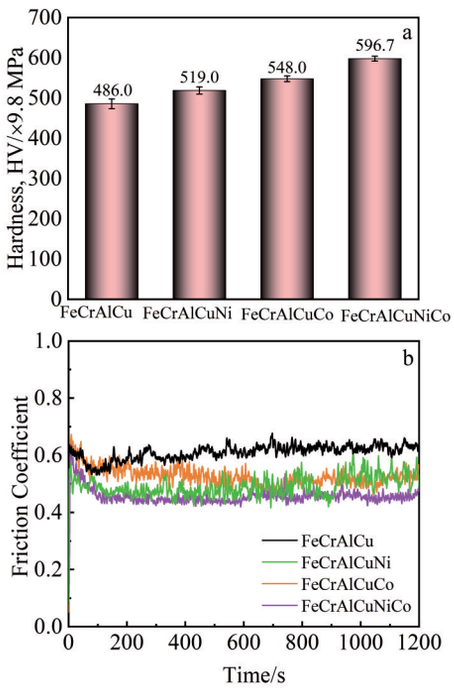

Fig.7 Hardness (a) and friction coefficient (b) of FeCrAlCu(Ni, Co) HEA coatings

FeCrAlCu, FeCrAlCuNi, FeCrAlCuCo, and FeCrAlCuNiCo HEA coatings is 0.59, 0.52, 0.47, and 0.45, respectively. The friction coefficient of FeCrAlCuNiCo HEA coating is the smallest. In FeCrAlCu HEAs, the introduction of Ni and Co elements can refine the grains owing to their high melting points and their contribution to the strengthening effect of grain boundaries. The grain boundaries effectively hinder the migration of dislocations and increase the strength. In the fine-grained structure, the dislocation movement is greatly hindered by the grain boundaries, leading to the higher density of dislocations, which in turn enhances the hardness of the material. Generally, the hardness and wear resistance are positively correlated, i. e., the higher the hardness, the better the abrasion resistance. Thus, the hardness is an important factor affecting the abrasion resistance[25–26].

Fig. 8 shows SEM images of wear marks of FeCrAlCu(Ni, Co) HEA coatings. It can be seen that the surface of FeCrAlCu HEA coating is relatively rough, and some long and narrow furrows can be seen along the sliding direction. A small amount of lamellar stratification and a large number of spalling pits can also be observed. When Ni and Co are separately added into HEA coating, the furrows on the coating surface are reduced and lamellar stratification barely exists. After simultaneous addition of Ni and Co, the coating surface becomes obviously smooth, the furrows become shallow and less, and the number of adhesive layers is also obviously reduced. These phenomena all indicate that when Ni and Co are simultaneously added, the wear mechanism of the FeCrAlCuNiCo HEA coating surface changes, which decreases the friction coefficient of the FeCrAlCuNiCo HEA coating. It can be concluded that the wear mechanism of FeCrAlCu(Ni, Co) HEA coatings is mainly adhesive wear, abrasive wear, and delamination wear.

Fig. 9 shows SEM images of the wear debris on FeCrAlCu(Ni, Co) HEA coatings. Flaky particles and fine equiaxed particles can be observed in the wear debris of all FeCrAlCu(Ni, Co) HEA coatings, presenting no significant difference. The flaky debris is produced due to the peeling phenomenon of the friction layer from the wear surface, whereas the fine equiaxed debris is formed due to the

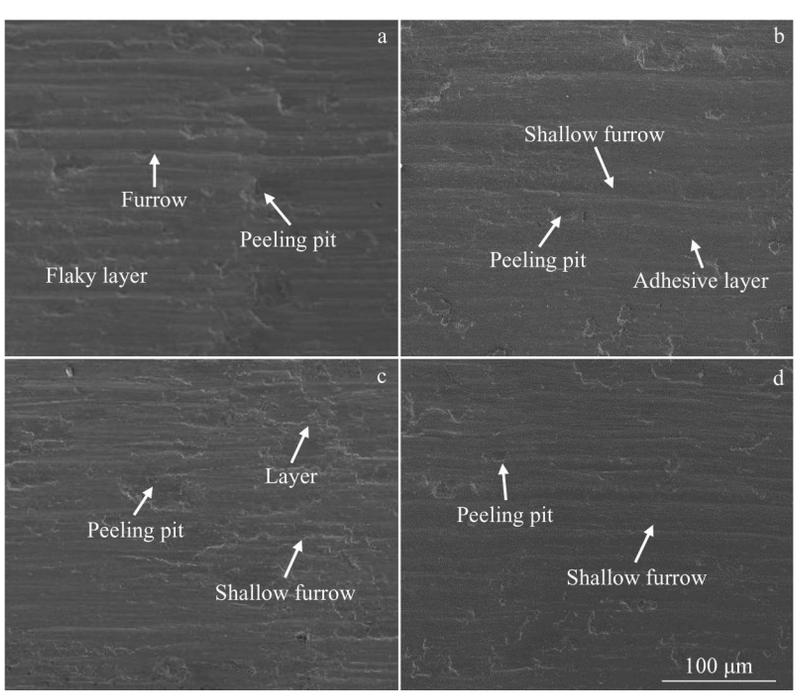

Fig.8 SEM images of wear marks of FeCrAlCu(Ni, Co) HEA coatings: (a) FeCrAlCu; (b) FeCrAlCuNi; (c) FeCrAlCuCo; (d) FeCrAlCuNiCo

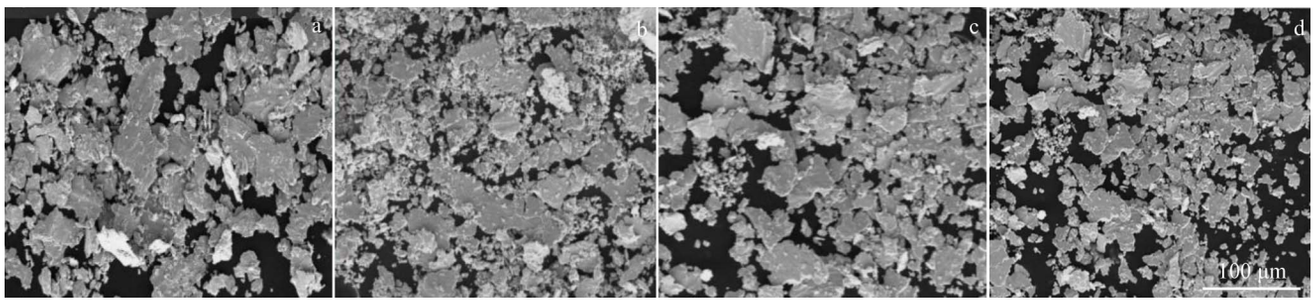

Fig.9 SEM images of wear debris on FeCrAlCu(Ni, Co) HEA coatings: (a) FeCrAlCu; (b) FeCrAlCuNi; (c) FeCrAlCuCo; (d) FeCrAlCuNiCo

fragmentation of the flaky debris or abrasive wear. Fig. 9d shows SEM image of the abrasive chips on the FeCrAlCuNiCo HEA coating. It can be found that with the simultaneous addition of Ni and Co atoms, the abrasive chips on the FeCrAlCuNiCo HEA coating gradually become smaller and are more uniformly distributed, which is mainly due to the higher hardness and strength of the FeCrAlCuNiCo HEA coating. The tearing force is reduced in the friction process, and plastic deformation hardly occurs. When the wear shear point locates in the coating material, the coating will not tear and transfer. After repeated grinding by the friction pair, the lamellar grinding chips become smaller. Fig. 10 shows EDS element mappings and EDS spectrum of the wear debris in Fig. 9d. It can be found that the wear debris of the FeCrAlCuNiCo HEA coating contains a small amount of O, and a fragile oxide layer forms on the coating surface during friction process. When the oxide layer is subjected to friction and pressure, it may flake off to form wear debris. It is worth noting that this fragile oxide layer is not formed by oxidization reaction occurring in the friction process.

Fig. 11 shows the three-dimensional friction morphologies of the FeCrAlCu(Ni, Co) HEA coatings prepared by laser

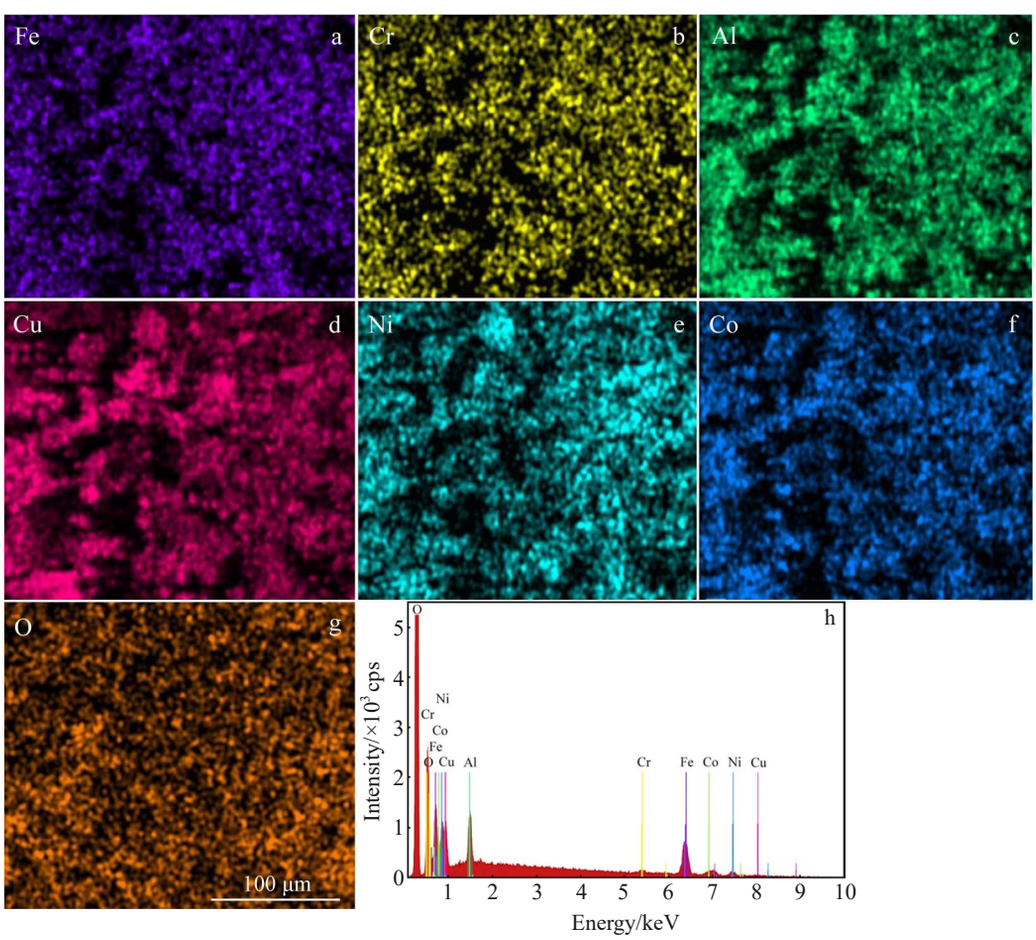

Fig.10 EDS element mappings (a–g) and EDS spectrum (h) of wear debris on FeCrAlCuNiCo HEA coating: (a) Fe; (b) Cr; (c) Al; (d) Cu; (e) Ni; (f) Co; (g) O

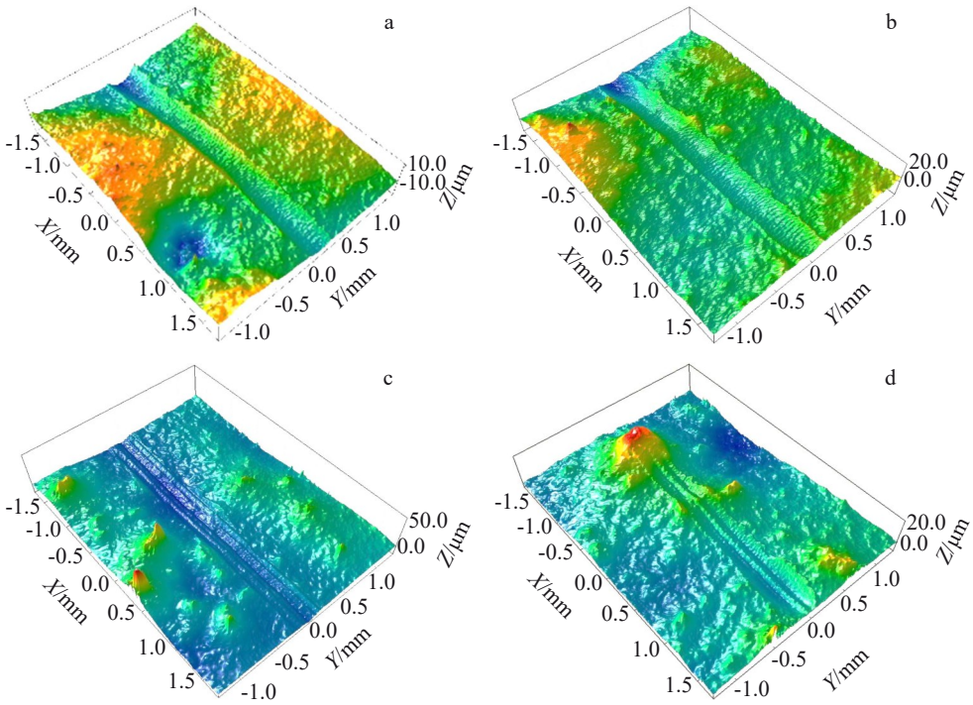

Fig.11 Three-dimensional friction morphologies of FeCrAlCu(Ni, Co) HEA coatings: (a) FeCrAlCu; (b) FeCrAlCuNi; (c) FeCrAlCuCo; (d) FeCrAlCuNiCo

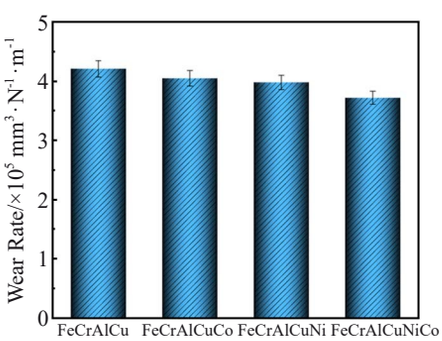

Fig.12 Wear rates of FeCrAlCu(Ni, Co) HEA coatings

remelting. The calculated wear rates of the FeCrAlCu(Ni, Co) HEA coatings are shown in Fig.12. The wear rates are 4.21×10^{-5}, 4.05×10^{-5}, 3.98×10^{-5}, and 3.72×10^{-5} $mm^3\cdot N^{-1}\cdot m^{-1}$ for FeCrAlCu, FeCrAlCuNi, FeCrAlCuCo, and FeCrAlCuNiCo HEA coatings, respectively. Therefore, the wear rate of FeCrAlCuNi, FeCrAlCuCo, and FeCrAlCuNiCo HEA coatings decreases by 45%, 38%, and 32%, respectively, compared with that of FeCrAlCu HEA coating. It can be concluded that FeCrAlCuNiCo HEA coating prepared by laser remelting shows good wear resistance.

3 Conclusions

1) The phase structure of FeCrAlCu(Ni, Co) HEA coatings synthesized by laser remelting is composed of simple bcc and fcc phases, and the intensity of diffraction peaks of bcc and fcc phases in FeCrAlCuNiCo HEA coating reaches the maximum when Ni and Co elements are simultaneously added.

2) The microstructure of FeCrAlCu(Ni, Co) HEA coatings synthesized by laser remelting is composed of columnar dendrites of bcc structure and intergranular dendrites of fcc structure. With the addition of Ni and Co, the columnar dendrites in the coating are refined.

3) When Ni and Co are added, the hardness of FeCrAlCu HEA coating increases. When Ni and Co are simultaneously added, the hardness of FeCrAlCuNiCo HEA coating reaches the maximum of 5847.7 MPa, the friction coefficient is 0.45, and the wear rate is 3.72×10^{-5} $mm^3\cdot N^{-1}\cdot m^{-1}$.

References

1 Yeh J W, Chen S K, Lin S J *et al. Advanced Engineering Materials*[J], 2004, 6(5): 299

2 Cantor B, Chang I T H, Knight P *et al. Materials Science & Engineering A*[J], 2004, 375–377: 213

3 Chen Guojin, Zhang Chong, Tang Qunhua *et al. Rare Metal Materials and Engineering*[J], 2015, 44(6): 1418 (in Chinese)

4 Sha Minghong, Wang Shuang, Li Shengli *et al. Rare Metal Materials and Engineering*[J], 2023, 52(11): 3685

5 Li Haozhe, Li Xiaolin, Jin Chi *et al. Journal of Materials Science & Technology*[J], 2023, 156: 241

6 Luo H, Zou S, Chen Y *et al. Corrosion Science*[J], 2020, 163: 108287

7 Li Wensheng. *Development of a New Type of High Alumina Bronze and Its Mechanism of Friction, Wear, Corrosion and Wear*[D]. Lanzhou: Lanzhou University of Technology, 2006 (in

Chinese)
8 Shi Y, Collins L, Feng R *et al. Corrosion Science*[J], 2018, 133: 120
9 Lu K, Zhu J, Guo D *et al. Coatings*[J], 2022, 12: 1023
10 Chen M, Lan L, Shi X *et al. Journal of Alloys and Compounds*[J], 2019, 777: 180
11 Wang M, Lu Y, Zhang G H *et al. Vacuum*[J], 2021, 184: 109905
12 Ge Feiyu, Yuan Haoming, Gao Qi *et al. Journal of Alloys and Compounds*[J], 2023, 949: 169741
13 Miao Junwei, Yao Hongwei, Wang Jun *et al. Journal of Alloys and Compounds*[J], 2022, 894: 162380
14 Cao Chenjie, Wang Yanfang, Zhang Cunxiu *et al. Rare Metal Materials and Engineering*[J], 2023, 52(4): 1439 (in Chinese)
15 Zhang Chong, Wu Bingqian, Wang Qianting *et al. Rare Metal Materials and Engineering*[J], 2017, 46(9): 2639 (in Chinese)
16 Liu Jingzhou, Liu Hongxi, Di Yingnan *et al. China Surface Engineering*[J], 2020, 33(6): 118 (in Chinese)
17 Shi F K, Zhang Q K, Xu C *et al. Optics & Laser Technology*[J], 2022, 151: 108020
18 Zou Y M, Qiu Z G, Huang C J *et al. Surface & Coatings Technology*[J], 2022, 434: 128205
19 Feng Li, Yang Weijie, Ma Kai *et al. The Chinese Journal of Nonferrous Metals*[J], 2023, 33(2): 490 (in Chinese)
20 Wang Yongdong, Gong Shulin, Chang Mengyang *et al. Transactions of the China Welding Institution*[J], 2024, 45(3): 107 (in Chinese)
21 Wang Y, Lu X, Yuan N *et al. Journal of Alloys and Compounds*[J], 2020, 849: 156
22 Feng Li, Yang Weijie, Ma Kai *et al. Materials Technology*[J], 2022, 37(13): 2567
23 Feng Li, Wang Jun, Wang Guiping *et al. Rare Metal Materials and Engineering*[J], 2021, 50(11): 3987 (in Chinese)
24 Zhou Y J, Zhang Y, Wang F J *et al. Applied Physics Letters*[J], 2008, 92(24): 299
25 Zhao Yanchun, Song Haizhuan, Ma Huwen *et al. Rare Metal Materials and Engineering*[J], 2024, 53(1): 102 (in Chinese)
26 Chen Di, Guan Yajie, Jin Guo *et al. Surface and Coatings Technology*[J], 2023, 461: 129447

激光重熔合成FeCrAlCu(Ni, Co)高熵合金涂层组织与耐磨性能

马　凯[1,2]，冯　力[1,2]，赵燕春[1,2]，刘建军[1,2]
(1. 兰州理工大学 材料科学与工程学院，甘肃 兰州 730050)
(2. 兰州理工大学 省部共建有色金属先进加工与再利用国家重点实验室，甘肃 兰州 730050)

摘　要：通过冷喷涂辅助激光重熔合成高熵合金涂层，在45#钢表面制备FeCrAlCu、FeCrAlCuNi、FeCrAlCuCo和FeCrAlCuNiCo高熵合金涂层。结果表明，这4种高熵合金涂层均由面心立方+体心立方相构成，涂层的组织由柱状树枝晶构成。随着Ni、Co元素的同时添加，涂层中的柱状树枝晶晶粒逐渐细化。FeCrAlCuNiCo高熵合金涂层的摩擦性能最佳，涂层的硬度为5847.7 MPa，摩擦因数为0.45，磨损率为3.72×10^{-5} $mm^3\cdot N^{-1}\cdot m^{-1}$。磨损机制为粘着磨损和磨粒磨损。

关键词：激光重熔；高熵合金涂层；磨损机制；耐磨性

作者简介：马　凯，男，1995年生，博士生，兰州理工大学材料科学与工程学院，甘肃 兰州 730050，E-mail：mkysys131477@163.com